Applied Acoustics 119 (2017) 1–8

Contents lists available at ScienceDirect

Applied Acoustics

journal homepage: www.elsevier.com/locate/apacoust

Modeling of random ground roughness effects by an effective impedance and application to time-domain methods

Olivier Faure [a,*], Benoit Gauvreau [a], Fabrice Junker [b], Philippe Lafon [a], Christophe Bourlier [c]

[a] Institut français des sciences et technologies des transports, des aménagements et des réseaux (Ifsttar), Laboratoire d'acoustique environnementale (LAE), Centre de Nantes, Route de Bouaye, CS4, 44344 Bouguenais Cedex, France
[b] EDF Lab Paris-Saclay, Département Analyses en Mécanique Avancée (AMA), 7 boulevard Gaspard Monge, 91120 Palaiseau, France
[c] Polytech Nantes, Télédetection team, Rue Christian Pauc, La Chantrerie, BP 50609, 44306 Nantes, France

ARTICLE INFO

Article history:
Received 7 June 2016
Received in revised form 21 November 2016
Accepted 29 November 2016
Available online 19 December 2016

Keywords:
Ground effect
Random ground roughness
Effective impedance
Time-domain
Numerical models

ABSTRACT

Natural grounds can exhibit small scale geometric irregularities, compared to the acoustic wavelength, known as ground roughness. This roughness has a noticeable effect on sound pressure levels and produces a surface wave. In the context of prediction methods improvement for outdoor sound propagation, using an effective impedance appears to be an useful approach to model the effects of surface roughness. Two time-domain numerical methods are considered: finite difference schemes (FDTD), and the transmission line modeling (TLM) method. An effective impedance model for random ground roughness defined by a roughness spectrum, called the SPM model, is exposed. The efficiency of this model for taking into account the mean effects of random roughness on sound pressure levels and for modeling the roughness-induced surface wave is shown, by comparing with results of TLM simulations of propagation above random rough grounds. The direct implementation of the SPM model as a boundary condition in both TLM and FDTD methods is then studied. This approach allows the modeling of ground roughness effects in numerical methods without having to mesh finely the ground roughness profile, allowing easier and faster computations, and more accurate predictions for future impact studies in environmental acoustics.

1. Introduction

The acoustical impact of industrial or transport installations on the environment is often estimated using simplified engineering methods. These methods need to be validated and fine tuned using reference results which can be experimentally or numerically obtained.

With the increase in computing power, the interest for the application of time-domain numerical methods to outdoor sound propagation has risen over the past years, *e.g.* see Refs. [1–4]. These methods are relevant as they can take into account most of the physical phenomena encountered during propagation, such as micro-meteorological effects (wind and temperature gradients, atmospherical turbulence) and ground effects, leading to very accurate numerical results for outdoor sound propagation.

Considering the ground effects, the interaction of the sound wave with a flat absorbing ground can be taken into account by transposing a frequency-domain boundary condition into the time-domain [5,6]. Realistic situations often involve irregular grounds with non-flat profiles. Ground irregularities with a topographic scale such as hills may be modeled using curvilinear coordinates solvers [7,8]. However natural grounds may also exhibit smaller geometry irregularities, whose characteristic size is inferior to the wavelength, known as ground roughness. Ground roughness produces a scattering of the sound wave that modifies the ground effect resulting from the interference between the direct and the ground-reflected wave. Ground roughness also leads to the formation of a surface wave [9,10].

This work focuses on the modeling of the effects of ground roughness in time-domain numerical methods for sound propagation, particularly the Finite Difference Time-Domain (FDTD) and Transmission Line Modeling (TLM) methods. Some difficulties arise when considering rough grounds, and the modeling of the ground profiles is not straightforward. First, the roughness may only be known statistically. Secondly, refining meshes at the boundaries in time-domain methods induces higher computation times (refining meshes could also be tricky regarding the introduction of phase error and artificial reflections at the transition zones between coarse and refined parts). To circumvent these difficulties, the

* Corresponding author.
E-mail address: oliv.fau@gmail.com (O. Faure).

http://dx.doi.org/10.1016/j.apacoust.2016.11.019
0003-682X/

effective impedance approach is considered: the effects of roughness on sound propagation are taken into account by considering a flat surface with a modified impedance boundary condition. Recently, the effective impedance approach has been used to model rough sea profiles in order to study numerically the propagation of noise generated by offshore wind farms [11]. Past works concern the effective impedance model proposed by Attenborough et al., that takes into account a roughness formed by small scatterers along the propagation path [12]. This model is known as the boss model, and the corresponding effective impedance is function of the geometry and spacing of the scatterers. Heuristic extensions of this model have been validated by reduced scale laboratory experiments [13,14,10] and outdoor measurements over agricultural surfaces such as plowed grounds [15]. Furthermore, the possibility and the interest to use this effective impedance model in time-domain numerical models was shown in Faure et al. [16].

In the present paper, a new effective impedance model for surface roughness is applied and tested for our specific application. Called the SPM model and originating from works in electromagnetism, it allows the modeling of the random roughness effects. The effective impedance is then expressed in function of the roughness spectrum of the height profile.

First, Section 2 exposes the boss model formalism and the SPM effective impedance model. The Gaussian roughness spectrum, which can be used to express the SPM effective impedance model, is also defined. In Section 3, TLM simulations of middle-range propagation above random rough grounds are performed, and the results are compared to analytical results with effective impedance in order to validate the accuracy of the SPM model for sound pressure levels predictions. The ability to model the roughness-induced surface wave using this effective impedance is also validated. Section 4 demonstrates the possibility and the interest to use the SPM effective impedance as a boundary condition in time-domain methods. The way to proceed for the implementation of the effective impedance in TLM and FDTD methods is exposed, and simulations are performed. Finally, in Section 5, the main results of this work are highlighted and concluding remarks are drawn.

2. Effective impedance models for random roughness

The effective impedance approach allows to model a rough ground by a perfectly flat ground with a modified impedance condition taking into account the effects of roughness on sound propagation. The effective impedance is expressed as a function of the roughness parameters. Then, using an effective impedance, sound levels above a rough ground can be estimated with simple models for propagation above a flat impedance ground with an homogeneous atmosphere, such as the well known Weyl-Van der Pol formula [17,18].

2.1. Boss model formulation for deterministic roughness

The boss effective impedance model proposed by Attenborough and Taherzadeh [19], based on Tolstoy's boss model [20] and Twersky's work [21], allows to calculate an effective impedance Z_{eff} (or an effective admittance $\beta_{\text{eff}} = 1/Z_{\text{eff}}$) for a set of semi-cylindrical scatterers, as shown in Fig. 1.

The effects of roughness are taken into account as a correction to the surface admittance β_S, and Z_{eff} is given by:

$$1/Z_{\text{eff}} = \beta_{\text{eff}} = \beta_S + \beta_R \tag{1}$$

where $\beta_S = 1/Z_S$. The base impedance Z_S for the flat surface can be evaluated using several models from the literature, such as the Delany-Bazley or Miki models, the Zwikker and Kosten model or the Attenborough model (these common ground impedance models are described in Attenborough et al. [22] for example). Hard-backed layer correction (thickness effect) can also be applied for the expression of Z_S [23]. The correction β_R is function of the angles θ_i and ϕ, the frequency, and other parameters depending of the scatterers' size, shape and spacing. These parameters and the exact formulation of β_R can be found in Boulanger et al. [12]. The model is valid for wavelengths larger than the roughness characteristic size, such as $k_0 h < k_0 b \leqslant 1$ where h is the scatterers' height ($h = a$ for the case of semi-cylindrical scatterers), and k_0 the wave number.

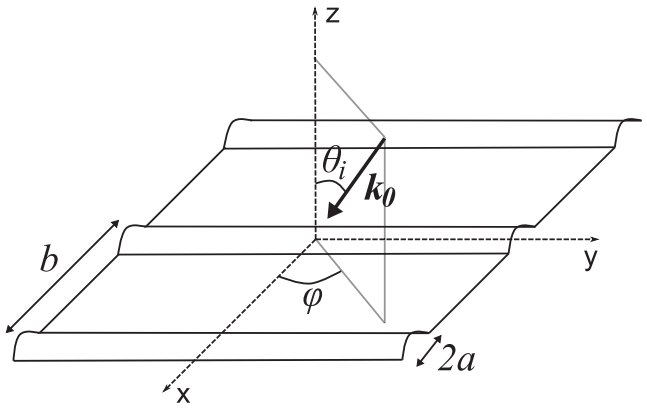

Fig. 1. Wave vector $\mathbf{k_0}$ incident to a surface containing cylinders of radius a and mean center-to-center spacing b [12].

2.2. SPM model for random roughness

An effective impedance model for sound propagation above hard randomly-rough surfaces was first developed by Watson and Keller [24,25]. This model is obtained using the Small Perturbation Method (SPM). It also found applications in the field of electromagnetic waves propagation above rough surfaces, such as the surface of the sea in the works of Brelet and Bourlier [26].

A 2D rough surface showing a small and slowly-varying roughness with $| k_0\zeta\cos(\theta_i) | < 1$ and $| \partial\zeta/\partial x | < 1$ is considered, as shown in Fig. 2. In this figure $\mathbf{k_0}$ and its modulus $| k_0 | = 2\pi f/c_0$ are respectively the wave vector and the wave number in the air, with c_0 the sound speed in the air, $\zeta(x)$ is the height profile, θ_i is the angle of incidence, Z_0 is the characteristic impedance of the air and Z_S is the impedance of the surface.

Under this assumption, it is thus possible to perform finite expansions of the Neumann boundary condition and the Green's function for a point source above the profile ζ. Then, the scattered field above the rough profile is modeled from a boundary integral formulation. A mean value of this integral is calculated using the Dyson equation and the Feynman diagram formalism [27]. Finally after using the Bourret approximation and some cumbersome manipulations [26,28], it is possible to derive an effective impedance from an equivalent reflection coefficient, in which the roughness effect is accounted for. This effective impedance is function of the roughness spectrum W of the surface. This roughness spectrum is defined as the Fourier Transform of the autocorrelation function of the surface height profile ζ (also defined as the spectral density of ζ), as follows:

$$W(k) = \int_{-\infty}^{+\infty} \exp(-2i\pi kx) C_\zeta(x) dx \tag{2}$$

with $C_\zeta(x) = \langle \zeta(x_1)\zeta(x_1 + x) \rangle$ the autocorrelation function of $\zeta(x)$.

The obtained effective impedance (or effective admittance) accounts for the mean effects of the random roughness on the

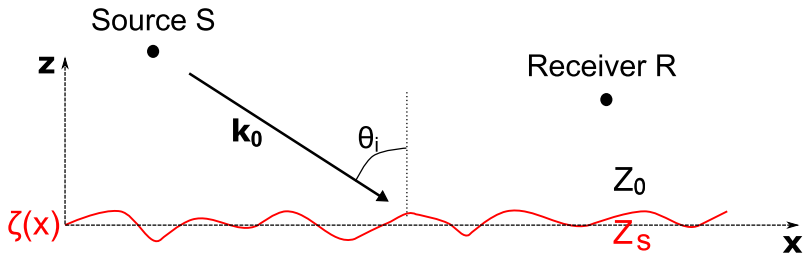

Fig. 2. Wave vector $\mathbf{k_0}$ incident to a rough surface ζ.

wave propagation. For a 2D acoustically hard (Neumann boundary condition) rough surface, the effective admittance is expressed by:

$$\beta_R^*[\kappa = k_0 \sin(\theta_i)] = \int_{-\infty}^{+\infty} \frac{d\kappa'}{k_0 k_z(\kappa')} \left(k_0^2 - \kappa\kappa'\right)^2 W(\kappa - \kappa') \tag{3}$$

with $k_z^2 = k_0^2 - \kappa^2, \kappa = k_0 \sin(\theta_i)$ and W the roughness spectrum of the surface. The integrand in Eq. (3) has an integrable singularity at $\kappa' = 0$ due to the term $k_z(\kappa')^{-1}$. The formulation proposed by Brelet and Bourlier [26] is then used in order to remove this singularity and facilitate the numerical integration.

This model as been extended to the case of an impedance rough surface [29,28]. Similarly to the boss model formulation, for a random rough absorbing surface the effects of roughness are also modeled as a correction of the surface admittance β_S. The effective impedance Z_{eff} is then given by:

$$1/Z_{\text{eff}} = \beta_{\text{eff}} = \beta_S + \beta_R^* \tag{4}$$

Here again, the base impedance Z_S can be expressed by a common ground impedance model for outdoor sound propagation, as exposed in Section 2.1. One should note that this SPM model given by Eq. (4) was derived under the assumption that $\beta_S \ll 1$ [29].

Two more important remarks are to be taken into consideration when using an effective impedance approach and particularly this SPM model. Firstly, the effective impedance is valuable for calculating the mean acoustic pressure field. However, it should be noticed, that the effective impedance is not sufficient to entirely characterize the acoustic field. For instance, the total intensity denoted by $I = \langle pp^* \rangle$ is not equal to the coherent intensity $I_C = \langle p \rangle \langle p^* \rangle$ and can only be approximated using an effective impedance. Secondly, as it can be seen in Eq. (3), the effective impedance of a rough locally-reacting ground depends on the angle of incidence. For long-distance propagation and near-grazing incidence situations, the angle of incidence can be approximated to $\theta_i = \pi/2$ to get rid of the angle-dependency.

2.3. Definition of a Gaussian roughness spectrum

In the following, the SPM model given by Eqs. (3) and (4) will be tested and validated considering a Gaussian roughness spectrum for the expression of W. Considering this roughness spectrum, the autocorrelation function of the surface profile is supposed to be a Gaussian function, and the random roughness is defined by only two statistical parameters, as detailed below. However, this commonly used theoretical description of surface roughness does not always model the roughness of real outdoor surfaces very well. For example, an exponential autocorrelation function better describes profiles showing micro-roughness, and is well-suited to approximate the roughness behavior of cultivated soils [30]. A generalized power-law spectrum, providing a wide range coverage for different natural surfaces, was introduced by Li et al. [31]. Nevertheless, in a first approximation of outdoor surfaces modeling, the Gaussian roughness spectrum is chosen is this work because roughness profiles characterized by a Gaussian spectrum show a small and smooth curvature, which satisfies the conditions of application of the small perturbation method. The Gaussian roughness spectrum is defined in k-space by:

$$W(k) = \frac{\sigma_h^2 l_c}{2\sqrt{\pi}} e^{\frac{-k^2 l_c^2}{4}} \tag{5}$$

where σ_h is the standard-deviation of the height and l_c the correlation length [32]. Fig. 3 shows an example of a roughness profile characterized by a Gaussian spectrum.

3. Numerical validation of the SPM model for a random rough surface with a Gaussian spectrum

In this section, 2D numerical simulations of propagation above rough absorbing grounds defined by Gaussian spectra are performed. A Transmission Line Matrix (TLM) code is used to perform these simulations. Details about the TLM method and its application to outdoor sound propagation can be found in Refs. [33,6]. Through the numerical simulations, the ground profiles are

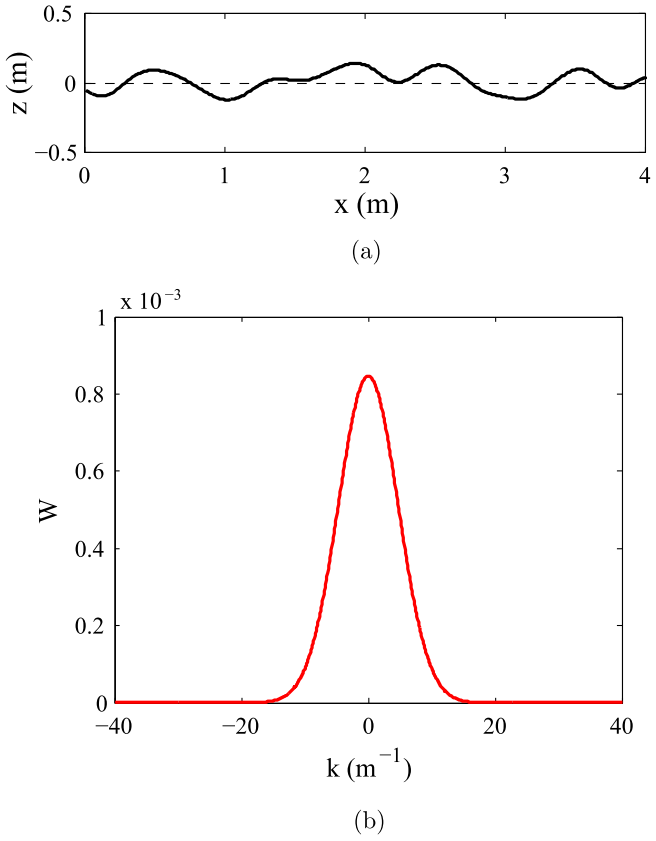

Fig. 3. (a) Example of a random roughness profile realization characterized by (b) a Gaussian spectrum defined by Eq. (5) with $\sigma_h = 0.1$ m et $l_c = 0.3$ m.

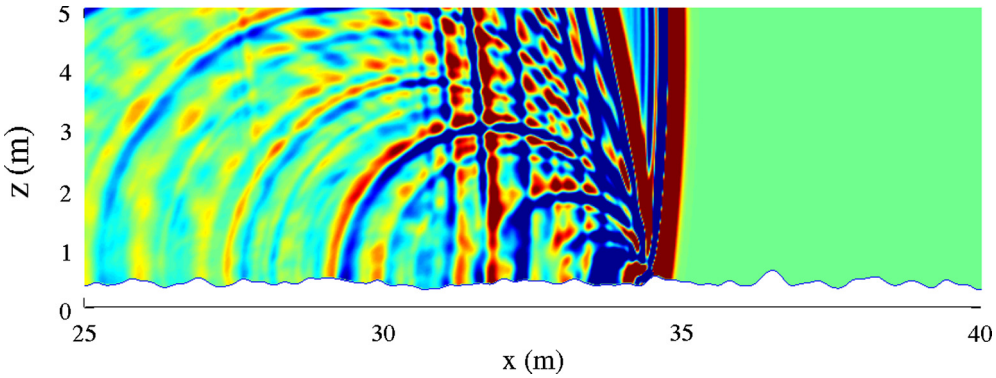

Fig. 4. Snapshot of the acoustic pressure at simulation time $t = 0.1$ s. A Gaussian pulse is propagating above a random realization of *ground 1*.

accurately meshed so the roughness effects are almost exactly modeled, but this is demanding important calculation resources. In order to assess the efficiency of the previously exposed SPM effective impedance for the modeling of roughness effects, analytical results obtained using the SPM effective impedance are compared to TLM numerical results.

3.1. Grounds definitions and TLM simulations

As the SPM model takes into account the mean effects of random roughness on sound propagation, several simulations of propagation above multiple realizations of random rough grounds must be carried out in order to obtain mean numerical results. The base impedance Z_S of the grounds is calculated using the Miki model with an hard-backed layer correction, accounting for an absorbing ground layer of air flow resistivity σ and thickness e. Two absorbing grounds showing roughnesses characterized by Gaussian roughness spectra are considered:

- *Ground 1*
  roughness mean properties (Gaussian spectrum): $\sigma_h = 0.05$ m, $l_c = 0.2$ m;
  impedance properties (Miki model with hard-backed layer): $\sigma = 200$ kN.s.m^{-4}, $e = 0.015$ m.
- *Ground 2*
  roughness mean properties (Gaussian spectrum): $\sigma_h = 0.07$ m, $l_c = 0.4$ m;
  impedance properties (Miki model and semi-infinite ground): $\sigma = 300$ kN.s.m^{-4}, $e = \infty$.

For each one of these two ground types, twenty 50 m-long realizations of rough grounds are generated [32]. TLM simulations of the propagation of a Gaussian pulse above each one of the 20 roughness realizations are performed for each ground type. The frequency content of the signal is 50–1000 Hz. For each simulation, the source is located at a height $H_S = 4$ m above the average height of the ground (0 m).

The spatial step of the simulations is $\Delta x = 0.01$ m in order to mesh the roughness with enough accuracy, and the time-step is $\Delta t = 2.05 \times 10^{-5}$ s. Fig. 4 shows a snapshot of the acoustic pressure above a random realization of the *ground 1* at the simulation time $t = 0.1$ s. An incoherent backscattered field is observed due to the random nature of the roughness.

3.2. Results in frequency domain

Results are studied in the frequency domain considering the relative attenuation spectra for two receivers located respectively at heights $H_{R1} = 4$ m and $H_{R2} = 0.3$ m, at an horizontal distance $d = 50$ m from the source. This configuration is chosen because it ensures attenuation spectra with large "ground dips" due to the interference between the direct and reflected fields, thus allowing a better exposure of the roughness effects. In Fig. 5, for each of the two ground types, the 20 attenuation spectra $\Delta L = L_{R1} - L_{R2}$ (blue[1] dashed curves) and their mean value (red curve) are plotted and compared to the analytical solution with the SPM effective impedance (green curve). This analytical solution is obtained using Eq. (4) for the expression of the impedance into the Weyl-Van der Pol formula for 2D cases [17]. The angle of incidence is $\theta_i = \pi/2$ for the calculation of the effective impedance and this analytical solution, as the considered source-receivers geometry is a case of near-grazing incidence. The analytical solution for a flat impedance ground is also plotted (black dashed curve) in order to assess for the effect of roughness.

The comparison of the numerical results over the rough grounds to the analytical result for a flat ground (black dashed curve) shows that the considered roughnesses have a noticeable effect on sound levels, even for the *ground 2* which has a more spread out and less pronounced roughness. Over the rough grounds (blue dashed curves), the first ground dips are shifted towards the lower frequencies, as if the grounds were more absorbing. This is in agreement with the results of Bashir et al. [10], when studying the effects of propagation over a rough surface formed by scatterers of constant geometry. For the two ground types, the analytical solution with effective impedance (green curve) fits accurately with the mean numerical results (red curve), hence showing that the SPM effective impedance model is efficient to take into account the mean effects of the roughness.

3.3. Results in time domain and surface wave

The SPM effective impedance model gives satisfactory results in the frequency domain. In order to study its efficiency to model the roughness-induced surface wave in the time domain, a third type of ground with a more pronounced roughness (then producing a stronger surface wave than *ground 1* and *ground 2*) has to be considered:

- *Ground 3*
  roughness properties (Gaussian spectrum): $\sigma_h = 0.1$ m, $l_c = 0.2$ m;
  impedance properties: Neumann condition.

[1] For interpretation of color in 'Figs. 5–7', the reader is referred to the web version of this article.

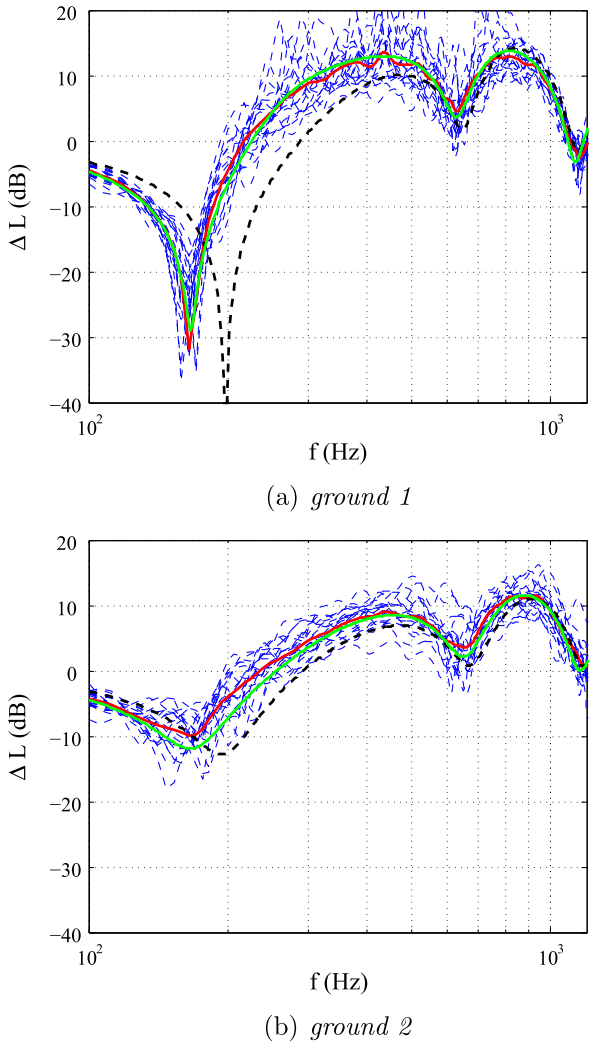

Fig. 5. Attenuation spectra ΔL at a distance $d = 50$ m above 20 realizations of each ground type. (– –) TLM results; (——) mean TLM result; (——) analytical solution with effective impedance (SPM model); (– –) analytical solution for the flat absorbing ground.

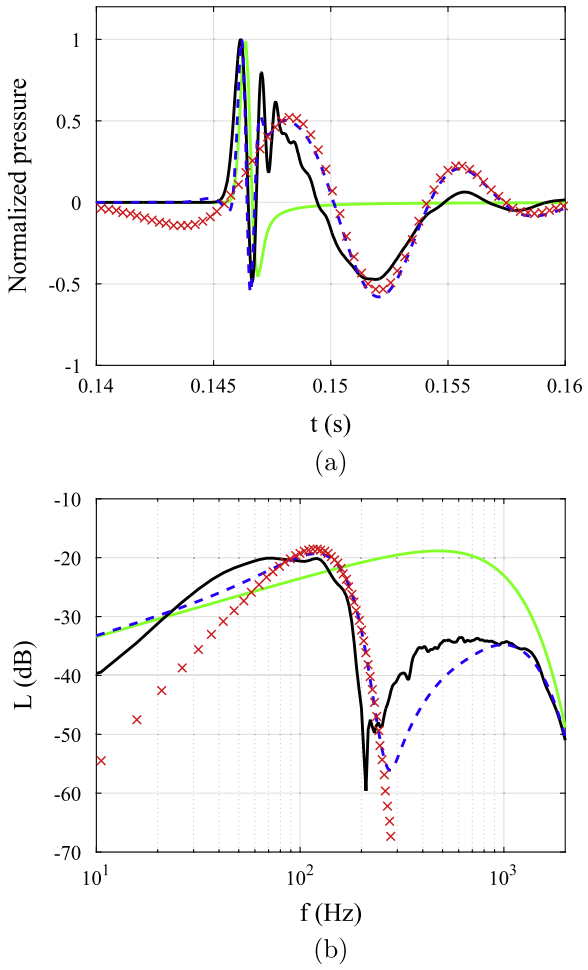

Fig. 6. (a) Time signal and (b) SPL spectrum at $d = 50$ m and $H_R = 1$ m above one random realization of *ground 3*. (——) TLM result; (– –) analytical solution with effective impedance (SPM model); (××) analytical solution for the surface wave contribution (SPM model); (——) analytical solution for the flat rigid surface.

The ground is considered perfectly rigid in order to focus on the surface wave only induced by the roughness, as a flat rigid ground does not produce any surface wave. Propagation of a Gaussian pulse above one 50 m-long realization of *ground 3* is simulated with the TLM method. The spatial and time steps are the same as in the previous simulations. The source is located at $H_S = 1$ m above the ground. The time signal obtained at a distance $d = 50$ m and a height $H_R = 1$ m is plotted in Fig. 6(a) (black curve). This result is compared to an analytical solution for the wave shape, obtained by inverse Fourier transform of the analytical result in the frequency domain given by the Weyl-Van der Pol formula with the SPM effective impedance model. The contribution of the surface wave only is also plotted (red doted curve). This solution in time-domain for the surface wave contribution is obtained by inverse Fourier transform of the analytical expression in frequency-domain for the surface wave term, which is given by Eq. (24) in [5]. Finally, the analytical solution for the flat rigid surfaces is also plotted (green curve) in order to appreciate how much the TLM solution is perturbed by the roughness.

A strong surface wave due to the roughness is observed on the TLM result as a low frequency tail (which is absent from the solution for the flat rigid surface). The shape of the analytical result with the SPM effective impedance is similar to the TLM result. The surface wave numerically observed is correctly modeled by the solution for the surface wave contribution (red dotted curve), although its amplitude is slightly overestimated. The frequency content of this roughness-induced surface wave is studied in Fig. 6(b). The energy maximum of the surface wave contribution calculated with the SPM model (red dotted curve) is noticeable for $f = 120$ Hz and fits exactly with the energy maximum in the lower frequencies of the TLM result (black curve). These results show that the SPM effective impedance is also suitable to accurately predict the roughness-induced surface wave.

4. Implementation of the SPM model in time-domain methods

In the previous section, it was shown through comparisons with numerical TLM simulations that the SPM effective impedance model is effective and accurate for the modeling of the random ground roughness effects. The use of the SPM model as a ground impedance boundary condition in the calculation methods for outdoor acoustics could be particularly helpful, as it would allow to perform calculations for complex cases of outdoor propagation (including ground roughness, flows, temperature gradients) without having to discretize the ground roughness profile. In order to demonstrate this, in this section the SPM effective impedance model is implemented in two time-domain methods: the TLM

method, already presented in the previous section, and the FDTD code named *Code_Safari*. The computations using the FDTD method are performed using 7-point centered finite-difference schemes and RK4 schemes. This FDTD method is detailed in Daude et al. [34].

4.1. Impedance boundary condition in time-domain models

In the frequency domain, the impedance condition at an absorbing boundary is given by:

$$P(\omega) = Z(\omega)V_n(\omega) \tag{6}$$

where $P(\omega)$ and $V_n(\omega)$ are respectively the Fourier transforms of the acoustical pressure and normal velocity at the boundary, and $Z(\omega)$ the impedance of the surface. In the time domain, this condition becomes a convolution product. In order to implement impedance models defined in frequency-domain, an efficient recursive convolution technique is used in both TLM and FDTD methods. This technique requires that the impedance is approximated by a sum of first order systems as follows:

$$Z(\omega) \approx Z^{\infty} + \sum_{k=1}^{K} \frac{a_k}{\lambda_k - j\omega} + \sum_{l=1}^{L} \frac{a_l}{\lambda_l - j\omega} + \frac{a_l^*}{\lambda_l^* - j\omega} \tag{7}$$

where a_k and λ_k are real coefficients, and a_l and λ_l are complex coefficients. The order of approximation is $N = K + 2L$.

The coefficients $a_{k,l}$ and $\lambda_{k,l}$ are then implemented as exposed in Dragna et al. [5] and Guillaume et al. [6] for the FDTD and TLM methods, respectively. It was shown by Cotté et al. [35] that the following conditions must be verified in order to ensure the stability of the computations:

$$\mathrm{Re}[\lambda_{k,l}]\Delta t < 2.5, \quad \mathrm{Im}[\lambda_{k,l}]\Delta t < 2.5 \tag{8}$$

4.2. Approximation of the effective impedances

The two effective impedances corresponding to *ground 1* and *ground 2* are approximated by Eq. (7) using the vector fitting method [36]. The approximation is performed for 100 frequencies between 50 Hz and 1200 Hz with a logarithmic step, for several order of approximation N such as $5 < N < 10$. For each value of N, the maximum values of $\mathrm{Re}[\lambda_{k,l}]\Delta t$ and $\mathrm{Im}[\lambda_{k,l}]\Delta t$ for poles identified by the vector fitting method are given in Tables 1 and 2, for *ground 1* and *ground 2* respectively. The chosen value of Δt corresponds to a spatial step $\Delta x = 0.05$ m in time-domain methods such as the FDTD in which the time-step and spatial step are linked by the CFL condition $\Delta t = C\Delta x/c_0$, with the CFL constant C set to $C = 0.9$ (a value ensuring the numerical stability of the simulations). The error of approximation by Eq. (7) on real and imaginary part of Z_{eff} is also given in the two tables. It is estimated as follows:

$$err(Z_{\mathrm{eff}}) = \left[\sum_f \left(Z_{\mathrm{eff}}(f)^{approx} - Z_{\mathrm{eff}}(f)^{exact} \right)^2 \Big/ \sum_f \left(Z_{\mathrm{eff}}(f)^{exact} \right)^2 \right]^2 \tag{9}$$

The two effective impedances are implemented in the FDTD and TLM codes, considering the values a_k, λ_k, a_l, and λ_l resulting of the vector fitting approximation that minimize both the values of $\mathrm{Re}[\lambda_{k,l}]\Delta t$ and $\mathrm{Im}[\lambda_{k,l}]\Delta t$ and the error of approximation. Thus for *ground 1*, according to Table 1 the results of the approximation at order $N = 6$ are considered. For *ground 2*, according to Table 2 the results of the approximation at order $N = 9$ are considered.

It is reminded that these two implemented effective impedances were calculated with $\theta_i = \pi/2$, and thus are only valid for simulations of grazing or near-grazing incidence situations.

4.3. FDTD and TLM simulations with SPM effective impedances

FDTD and TLM simulations are performed, considering flat grounds with SPM effective impedances accounting for random roughness and absorption of *ground 1* and *ground 2*. In both numerical methods, a spatial step $\Delta x = 0.025$ m is chosen (which is 2.5 times bigger than the spatial-step considered in Section 3). For the TLM and FDTD simulations, the time step is respectively $\Delta t = 5.1 \times 10^{-5}$ s and $\Delta t = 6.6 \times 10^{-5}$ s. The source-receivers geometry and configuration are the same as considered in the TLM simulations of Section 3.2, in which the ground roughness profile was meshed. In Fig. 7(a) and. (b), the attenuation spectra obtained by FDTD and TLM (black and blue curves, respectively) are compared to the mean result of TLM simulations performed in Section 3.2 (red curve) where the roughness profiles were accurately meshed and almost exactly modeled.

For these two cases, one can see a perfect agreement between the two numerical results with SPM effective impedance and the mean numerical result of Section 3.2. First, this shows that the effective impedances for the two grounds were correctly implemented in both time-domain models. Secondly, these results demonstrate the interest of using SPM effective impedance in numerical methods, as it allows to accurately take into account

Table 1
Approximation of the effective impedance corresponding to *ground 1* by vector fitting at order N.

N	K	$(\lambda_k\Delta t)_{max}$	L	$(Re[\lambda_l\Delta t])_{max}$	$(Im[\lambda_l\Delta t])_{max}$	err(Re[Z]) (%)	err(Im[Z]) (%)
5	3	1.45	1	0.08	0.46	1.47	1.37
6	6	2.1	0	0	0	0.61	1.18
7	3	95.7	2	0.3	0.3	0.03	1.16
8	4	6.23	2	0.28	0.25	0.29	1.06
9	5	4.48	2	0.29	0.33	0.35	1.02
10	6	3.28	2	0.33	0.28	0.18	0.70

Table 2
Approximation of the effective impedance corresponding to *ground 2* by vector fitting at order N.

N	K	$(\lambda_k\Delta t)_{max}$	L	$(Re[\lambda_l\Delta t])_{max}$	$(Im[\lambda_l\Delta t])_{max}$	err(Re[Z]) (%)	err(Im[Z]) (%)
5	3	3.29	1	0.27	0.11	0.45	3.76
6	4	3.78	1	0.04	0.12	0.32	3.21
7	3	2.42	2	0.17	0.12	0.42	2.66
8	4	3.79	2	0.15	0.17	0.13	1.87
9	3	0.99	3	0.66	1.35	0.12	1.61
10	4	4.3	3	0.13	0.26	0.11	1.75

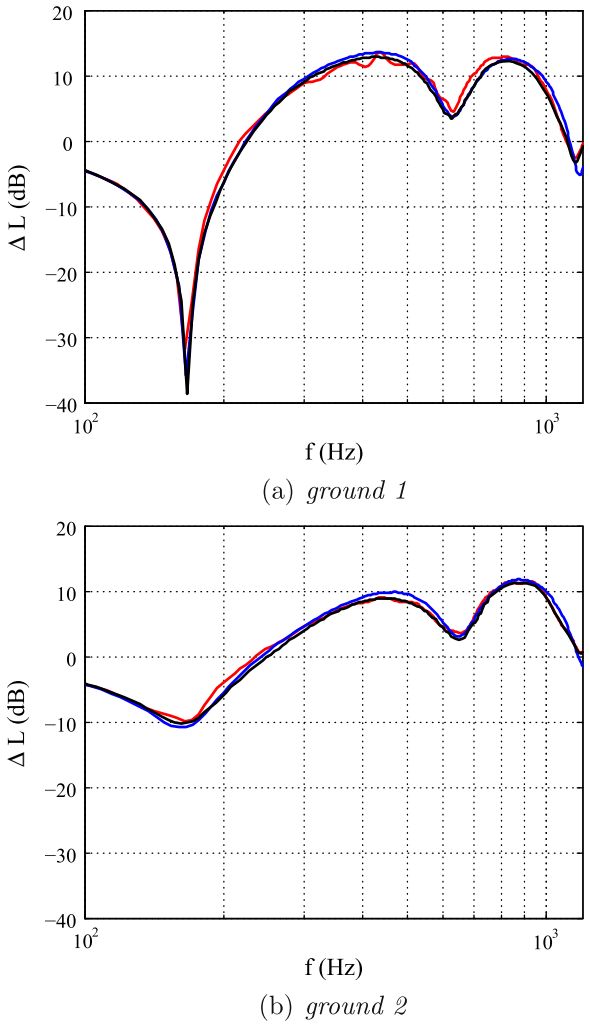

Fig. 7. Attenuation spectra ΔL at $d = 50$ m resulting from numerical simulations with SPM effective impedance. (—) FDTD result, (—) TLM result, (—) mean TLM result obtained in 3.2.

the effects of random ground roughness without exactly meshing the ground profile. Furthermore, bigger spatial steps can be considered, thus leading to shorter calculation times, and thus to long-range outdoor sound propagation applications.

5. Concluding remarks

Ground roughness has noticeable effects on outdoor sound propagation: (i) it shifts the ground dip due to the ground effect towards the lower frequencies and (ii) it leads to the formation of a surface wave. The boss model approach allows to express an effective impedance for a ground roughness formed by regular scatterers, such as semi-cylinders. In this paper, an effective impedance model for random roughness was developed. Using the Small Perturbation Method (SPM), it models the mean effects of random ground roughness characterized by a roughness spectrum, such as the Gaussian roughness spectrum which is defined by two statistical parameters. Just like the boss model formulation, for an absorbing ground, the ground roughness effect is modeled as a correction to the base admittance of the ground surface.

This SPM effective impedance model was validated numerically for middle-distance outdoor sound propagation cases. Two-dimensional TLM simulations of 50 m propagation above absorbing and rigid random rough grounds (whose roughness was defined by a Gaussian spectrum) were performed. The results were compared to analytical solutions calculated with the SPM effective impedance model, and showed that the SPM effective impedance accurately takes into account the mean effects of roughness on sound level spectra, and also correctly models the roughness-induced surface wave.

Then, the possibility and the interest to use the SPM effective impedance model at boundary conditions in time-domain numerical methods was shown. SPM effective impedances were implemented in FDTD and TLM codes by approximating the effective impedance by a sum of rational functions, using the vector fitting technique to identify the coefficients of these functions. FDTD and TLM numerical methods with SPM effective impedance have been proven to be efficient and useful for simulating complex middle-range propagation cases with time-domain methods, as they allow to take into account quite easily the mean effects of a statistically defined roughness. The ability to do that without meshing the roughness can also significantly reduce the computation time.

It should be pointed out that in order to be used in time-domain, an impedance model must be physically admissible and verify reality, causality and passivity conditions [37,38]. The Miki model with thickness effect was the base impedance model considered to derive the SPM effective impedance for the considered grounds using Eq. (4). Recent studies [39,40] showed that the Miki model is actually not physically admissible, and not the best suited model for long-range outdoor sound propagation predictions despite its common use. Nevertheless it gave satisfactory results within the frame of this work. Furthermore, this SPM effective impedance approach should still prove functional using more refined base impedance models, such as the slit pore model [22].

A promising application for effective impedance models and particularly for the SPM model would be to use them in engineering methods for long-range noise impact predictions. This would require experimental data to characterize roughness spectra of natural grounds. The model will be soon available in *Code_TYMPAN*, an open source software dedicated to outdoor sound engineering calculations [41]. Another application would concern propagation above the water for offshore wind farms, as roughness spectra have been studied for sea surfaces [42].

References

[1] Hornikx M, Waxler R, Forssn J. The extended Fourier pseudospectral time-domain method for atmospheric sound propagation. J Acoust Soc Am 2010;128(4):1632–46.
[2] Dragna D, Blanc-Benon P, Poisson F. Impulse propagation over a complex site: a comparison of experimental results and numerical predictions. J Acoust Soc Am 2014;135(3):1096–105.
[3] Guillaume G, Aumond P, Gauvreau B, Dutilleux G. Application of the transmission line matrix method for outdoor sound propagation modelling – Part 1: Model presentation and evaluation. Appl Acoust 2014;76(0):113–8.
[4] Van Renterghem T. Efficient outdoor sound propagation modeling with the finite-difference time-domain (FDTD) method: a review. Int J Aeroacoust 2014;13(5–6):385–404.
[5] Dragna D, Cotte B, Blanc-Benon P, Poisson F. Time-domain simulations of outdoor sound propagation with suitable impedance boundary conditions. AIAA J 2011;49:1420–8.
[6] Guillaume G, Picaut J, Dutilleux G, Gauvreau B. Time-domain impedance formulation for transmission line matrix modelling of outdoor sound propagation. J Sound Vib 2011;330(26):6467–81.
[7] Heimann D, Karle R. A linearized Euler finite-difference time-domain sound propagation model with terrain-following coordinates. J Acoust Soc Am 2006;119(6):3813–21.
[8] Hornikx M, Dragna D. Application of the Fourier pseudospectral time-domain method in orthogonal curvilinear coordinates for near-rigid moderately curved surfaces. J Acoust Soc Am 2015;138(1):425–35.
[9] Donato RJ. Model experiments on surface waves. J Acoust Soc Am 1978;63(3):700–3.
[10] Bashir I, Taherzadeh S, Attenborough K. Diffraction assisted rough ground effect: models and data. J Acoust Soc Am 2013;133(3):1281–92.

[11] Van Renterghem T, Botteldooren D, Dekoninck L. Airborne sound propagation over sea during offshore wind farm piling. J Acoust Soc Am 2014;135(2):599–609.
[12] Boulanger P, Attenborough K, Taherzadeh S, Waters-Fuller T, Li KM. Ground effect over hard rough surfaces. J Acoust Soc Am 1998;104(3):1474–82.
[13] Chambers JP, Sabatier JM. Recent advances in utilizing acoustics to study surface roughness in agricultural surfaces. Appl Acoust 2002;63(7):795–812.
[14] Boulanger P, Attenborough K. Effective impedance spectra for predicting rough sea effects on atmospheric impulsive sounds. J Acoust Soc Am 2005;117(2):751–62.
[15] Attenborough K, Waters-Fuller T. Effective impedance of rough porous ground surfaces. J Acoust Soc Am 2000;108(3):949–56.
[16] Faure O, Gauvreau B, Junker F, Lafon P. Effective impedance models for rough surfaces in time-domain propagation methods. In: Proceedings of inter-noise 2013, Innsbruck, Austria; 2013.
[17] Chandler-Wilde S, Hothersall D. Efficient calculation of the green function for acoustic propagation above a homogeneous impedance plane. J Sound Vib 1995;180(5):705–24.
[18] Attenborough K, Li KM, Horoshenkov K. Predicting outdoor sound. Taylor & Francis; 2006.
[19] Attenborough K, Taherzadeh S. Propagation from a point source over a rough finite impedance boundary. J Acoust Soc Am 1995;98(3):1717–22.
[20] Tolstoy I. Coherent sound scatter from a rough interface between arbitrary fluids with particular reference to roughness element shapes and corrugated surfaces. J Acoust Soc Am 1982;72(3):960–72.
[21] Lucas RJ, Twersky V. Coherent response to a point source irradiating a rough plane. J Acoust Soc Am 1984;76(6):1847–63.
[22] Attenborough K, Bashir I, Taherzadeh S. Outdoor ground impedance models. J Acoust Soc Am 2011;129(5):2806–19.
[23] Allard J, Atalla N. Propagation of sound in porous media: modelling sound absorbing materials 2e. John Wiley & Sons; 2009.
[24] Watson JG, Keller JB. Reflection, scattering, and absorption of acoustic waves by rough surfaces. J Acoust Soc Am 1983;74(6):1887–94.
[25] Watson JG, Keller JB. Rough surface scattering via the smoothing method. J Acoust Soc Am 1984;75(6):1705–8.
[26] Brelet Y, Bourlier C. SPM numerical results from an effective surface impedance for a one-dimensional perfectly-conducting rough sea surface. Prog Electromagn Res – PIER 2008;81:413–36.
[27] Bass FG, Fuks IM. Wave scattering from statistically rough surfaces: international series on natural philosophy, vol. 93. Oxford Pergamon Press; 2013.
[28] Brelet Y. Diffusion des ondes lectromagntiques par une surface rugueuse monodimensionnelle sous incidences modres et rasantes: application au domaine maritime. Ph.D. thesis. Nantes; 2008.
[29] Ishimaru A, Rockway JD, Lee S-W. Sommerfeld and Zenneck wave propagation for a finitely conducting one-dimensional rough surface. IEEE Trans Antennas Propag 2000;48(9):1475–84.
[30] Verhoest NE, Lievens H, Wagner W, Álvarez-Mozos J, Moran MS, Mattia F. On the soil roughness parameterization problem in soil moisture retrieval of bare surfaces from synthetic aperture radar. Sensors 2008;8(7):4213–48.
[31] Li Q, Shi J, Chen K-S. A generalized power law spectrum and its applications to the backscattering of soil surfaces based on the integral equation model. IEEE Trans Geosci Rem Sens 2002;40(2):271–80.
[32] Bourlier C, Pinel N, Kubické G. Method of moments for 2D scattering problems: basic concepts and applications. John Wiley & Sons; 2013.
[33] Hofmann J, Heutschi K. Simulation of outdoor sound propagation with a transmission line matrix method. Appl Acoust 2007;68(2):158–72.
[34] Daude F, Berland J, Emmert T, Lafon P, Crouzet F, Bailly C. A high-order finite-difference algorithm for direct computation of aerodynamic sound. Comput Fluids 2012;61:46–63.
[35] Cotté B, Blanc-Benon P, Bogey C, Poisson F. Time-domain impedance boundary conditions for simulations of outdoor sound propagation. AIAA J 2009;47(10):2391–403.
[36] Gustavsen B, Semlyen A. Rational approximation of frequency domain responses by vector fitting. IEEE Trans Power Deliv 1999;14(3):1052–61.
[37] Rienstra S. Impedance models in time domain including the extended Helmholtz resonator model. In: Proceedings 12th AIAA/CEAS aeroacoustics conference, Cambridge MA, USA, May 8 10, 2006, vol. 2686; 2006. p. 1 [Paper AIAA 2006].
[38] Dragna D, Blanc-Benon P. Physically admissible impedance models for time-domain computations of outdoor sound propagation. Acta Acust United Acust 2014;100(3):401–10.
[39] Kirby R. On the modification of Delany and Bazley fomulae. Appl Acoust 2014;86:47–9.
[40] Dragna D, Attenborough K, Blanc-Benon P. On the inadvisability of using single parameter impedance models for representing the acoustical properties of ground surfaces. J Acoust Soc Am 2015;138(4):2399–413.
[41] EDF. Code_TYMPAN: an open source software for acoustic propagation. URL <http://www.code-tympan.org>; 2016.
[42] Elfouhaily T, Chapron B, Katsaros K, Vandemark D. A unified directional spectrum for long and short wind–driven waves. J Geophys Res: Oceans (1978–2012) 1997;102(C7):15781–96.